

Nanomachining of mesoscopic graphite

P. Barthold, T. Lüdtkke, and R. J. Haug

Institut für Festkörperphysik, Leibniz Universität Hannover, Appelstr. 2, 30167 Hannover, Germany

(Dated: September 15, 2021)

An atomic force microscope is used to structure a film of multilayer graphene. The resistance of the sample was measured *in-situ* during nanomachining narrow trenches. We found a reversible behavior in the electrical resistance which we attribute to the movement of dislocations. After several attempts also permanent changes are observed.

PACS numbers: 73.63.-b, 73.22.-f, 73.23.-b, 81.07.-b

Atomic force microscopes (AFMs) are well known tools for imaging and for structuring. Besides other lithographic methods nanomachining with the AFM is a simple, but highly efficient way to design devices on the sub-micron level. By applying a high contact force between sample and AFM tip a permanent deformation of the sample's surface is obtained. Using this method different materials have been structured e.g. semiconductors^{1,2,3} and metals⁴.

Up to now the common technique to structure graphene is by etching.^{5,6,7} Graphene has drawn a great deal of attention since the discovery of free standing single layer graphite (so-called graphene) and its unique electronic properties.^{8,9,10,11} The motivation for the work presented here was to structure graphene via nanomachining with an AFM tip. In a first step we structured a thin film of graphite by nanomachining a trench through the half width of the sample. Hence the conducting area of the sample is reduced and thereby a constriction is formed. As we observed interesting reversible behavior in the resistance in this setup, in a second step we have cut another sample through the whole width to see similar effects.

The graphite samples used in this study are extracted from natural graphite¹² by exfoliation¹³ on a silicon substrate with a 300 nm SiO₂ layer. The thereby formed flake has a lateral dimension of a few micrometers and a thickness of about 10 nm (~ 30 atomic layers, assuming a lattice constant of 0.34 nm). The Ti/Au (9 nm/46 nm) electrodes are fabricated using standard electron beam lithography. After bonding the sample it is electrically contacted inside the AFM allowing *in-situ* measurements at room temperature. Figure 1 shows the general setup. A direct current of $I = 500$ nA is driven via two contacts through the sample while the voltage V is measured using the two remaining electrodes. For the measurements presented here we used an AFM tip that is coated with polycrystalline diamond on the tip-side. During the measurements we applied a force of approximately $0.5 \mu\text{N}$. Using such a high contact force the tip is moved with a velocity of about $0.5 \mu\text{m/s}$ half the way across the graphite flake as sketched by the white arrows in Fig. 1. The tip starts its movement left of the flake, moves about $2.2 \mu\text{m}$ through the flake and returns back to its starting position. Thus the tip scratches the sample in both directions. After five of those movements a distinct trench

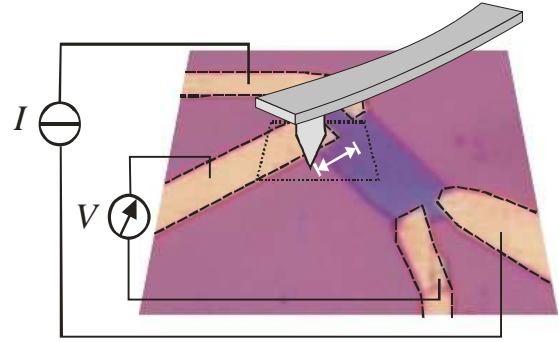


FIG. 1: Schematic drawing of the setup. The optical picture shows the graphite flake with four electrodes. A direct current is driven through the sample via two contacts while the voltage is measured using the other two electrodes. The AFM tip moves from left to right and to the left again while a high contact force is applied. The dashed square marks the region which is shown in Fig. 2(a) and (b).

is formed in the graphite film.

Figures 2(a) and (b) show two AFM pictures of the sample before and after nanomachining. A trench of about $2.2 \mu\text{m}$ is clearly visible in the graphite flake in Fig. 2(b). Figure 2(c) demonstrates the time evolution of the resistance while scratching the graphite film with the AFM tip. The time period when the tip moves on top of the graphite is marked grey in Fig. 2(c). At $t = 0$ s the resistance of the sample is about $R \approx 248 \Omega$. At $t \approx 15$ s when the tip is moved over the graphite for the first time (I) with the high contact force the resistance starts to increase. The resistance reaches its first maximum of $R \approx 258 \Omega$ at $t \approx 21$ s which coincides with the reversal point of the AFM tip movement. The resistance drops again to its original value by moving the tip back to the original starting position. When the tip applies a force to the graphite for the second time the resistance starts to rise again (II). This time the value rises up to about 275Ω . Afterwards the resistance drops to a value of 248Ω . As the AFM tip moves over the flake for the third time (III) the resistance increases to a value of about 277Ω . Now the resistance decreases to $R \approx 258 \Omega$, which is $\Delta R \approx 9 \Omega$ higher than the resistance in the beginning. The value after the third tip movement is the same as the maximum obtained during AFM run I, as in-

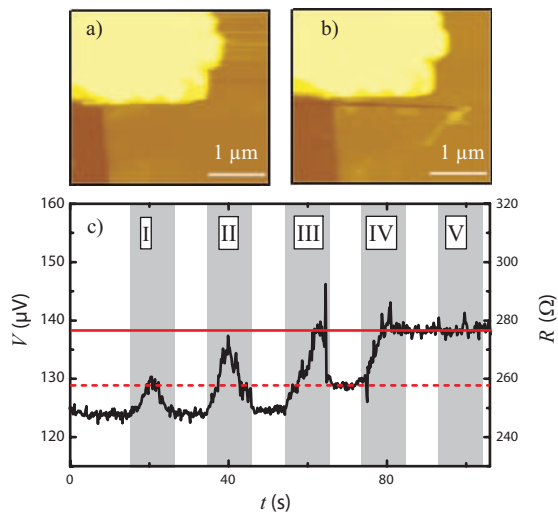


FIG. 2: Upper part: AFM images of the graphite flake with a height of about 10 nm. (a) Magnification of the interesting part as marked in Fig 1. (b) After nanomachining five times with the AFM tip. A clear trench in the graphite is visible. Its dimensions are $w_S \approx 2.2 \mu\text{m}$ and $l_S \approx 100 \text{ nm}$. (c) Time evolution of the resistance of the sample while the AFM tip applies a force to the graphite. The grey regions indicate when the tip actually moves on top of the graphite, the roman numerals count the number of movements. The dashed and solid vertical lines are guides to the eye to stress the similar resistances of the sample during different times of structuring.

indicated by the dashed line in Fig. 2(c) As the tip moves for the fourth time (IV) over the graphite, the resistance rises again to a value of about 277Ω . The same value is already reached during run II and III. But this time the resistance does not drop again instead it stays at a value of $R \approx 277 \Omega$. This resistance is kept even when the tip moves for a fifth time (V) on top of the graphite and stays at this value afterwards. Thus the resistance of the graphite film was permanently changed by $\Delta R \approx 29 \Omega$ using an AFM tip to structure it.

To explain this behavior we consider the following model: While the AFM tip is moved over the sample dislocations are induced along the trajectory of the movement of the tip. These dislocations modify the electronic properties of the sample. Thus the resistance of the sample rises during scratching. These dislocations then move to the edge of the sample where we assume that their influence on the electronic properties of the flake is only small. Grenall reported dislocation movement in smeared flakes of natural graphite.¹⁴ As observed by Williamson dislocations in graphite run parallel to the layer plane.¹⁵ Mainly they move to the edge of the flake or to cleavage steps. Hence bonds just destroyed by the AFM tip along the trajectory of the movement could close again and the transport properties get back to the original state, thus the resistance drops again to its original value.

As our sample consists of many layers, it seems reasonable to believe that during the first time the sample is

scratched (I) dislocations are induced only in the few upper layers and during the second time (II) dislocations are induced in more layers. This would explain the higher resistance during run II compared to I. As the resistance during run II is close to the value reached at the end, dislocations seem to be formed in most of the layers when scratching for the second time.

The defects induced during the second time of scratching could move again to the edge of the sample. Therefore the resistance drops (between II and III) to its original value. During the third time of scratching (III) a lasting deformation occurs for the first time. In a few layers the bonds destroyed by the AFM tip are not closed again and thereby influence the electronic properties of the sample permanently. During the fourth run (IV) all layers are cut through on a $2.2 \mu\text{m}$ long path along the sample. Thus the resistance keeps its value even when it is scratched for the fifth time. All bonds are destroyed along the trajectory of the movement of the AFM tip.

Using a simple classical resistance network model we find the following results: Knowing the geometry and measuring the resistance R of the sample with a four terminal setup we are able to calculate the specific resistance ρ :

$$\rho = R \cdot \frac{w \cdot h}{l}, \quad (1)$$

where l is the length in current direction, w the width orthogonal to the current direction, and h the height of the sample. The measured values are $R \approx 248 \Omega$, $l \approx 7.3 \mu\text{m}$, $w \approx 5.2 \mu\text{m}$, and $h \approx 10 \text{ nm}$. The resulting specific resistance is $\rho \approx 1.77 \cdot 10^{-6} \Omega\text{m}$, being comparable to the specific resistance $\rho \approx 1.2 \cdot 10^{-6} \Omega\text{m}$ reported by Powell et al. for natural graphite.¹⁶ Now we estimate the measured resistance during nanomachining using our simple equivalent circuit by dividing the sample into four parts: the part above the trench R_1 , the area beneath the trench R_3 , the manipulated part R_S , and the area right to the trench R_2 , therefore parallel to R_S . This leads to an overall resistance given by:

$$R_{res} = R_1 + \frac{R_S \cdot R_2}{R_S + R_2} + R_3. \quad (2)$$

Nanomachining changes the resistance by $\Delta R \approx 29 \Omega$. We now calculate an area of the flake that does not participate in electrical transport in the end and thereby explains the change in resistance. We use $w_S \approx 2.2 \mu\text{m}$ for the width of the trench. To determine the other dimension l_S^* we equate Eq. 2 with the resistance in the beginning ($R_{res} = 248 \Omega$) and in the end ($R_{res} = 277 \Omega$, $R_S \rightarrow \infty$). Together with Eq. 1 we find $l_S^* \approx 1.16 \mu\text{m}$ for the part of the sample which is nonconducting in the end. This model shows that not only the trench is insulating in the end, but the area nearby is as well influenced in its electrical transport properties, as the calculated l_S^* is about ten times larger than the measured l_S of the trench, clearly showing the limit of this classical model for a mesoscopic sample.

In this model the different resistances observed can be

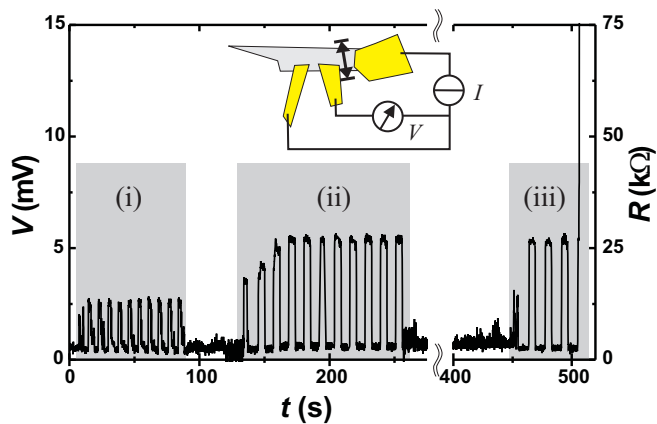


FIG. 3: Measurement of sample 2. The inset shows a sketch of the setup. The three gold electrodes and the graphite flake are shown. The arrow indicates the trajectory of the tip moved over the whole sample. The *in-situ* measurement of voltage is shown on the left axis and the corresponding resistance on the right axis. In each interval (i), (ii), and (iii) a different contact force is applied to the sample. At $t \approx 510$ s the resistance rises to the measurable limit. Hence the graphite is cut through.

described by assuming the following dimensions of the resistances in the equivalent circuit: $l_1 \approx 180$ nm, $w_1 \approx 5.2$ μm , $l_3 \approx 5.9$ μm , and $w_3 \approx 5.2$ μm for the upper and lower part R_1 and R_3 , respectively. The resistances in the middle are described by: $w_S \approx 2.2$ μm and $l_S^* \approx 1.16$ μm for the left area R_S , and for the region right to the structured part: $l_S^* = l_2 \approx 1.16$ μm and $w_2 \approx 3$ μm . For $R_S \rightarrow \infty$ Eq. 2 leads to $R \approx 277$ Ω as measured in the end. During nanomachining (e.g. during run I) we have to assume a height of $h_S = 5$ nm for R_S instead of $h_S = 10$ nm at the beginning and $h_S = 0$ nm at the end.

In Fig. 3 the measured resistance for another sample is shown. In this case we use a three terminal setup as sketched in the inset to drive a current through the device and to measure the voltage. The sample is structured in three different intervals, during each interval the tip is moved eleven times through the sample with different forces: < 0.1 μN , about 1 μN , and approximately 2 μN . In the last interval during the fourth time of moving the tip, the resistance reaches the detectable limit. Hence the graphite film is cut through. The dramatic change in the resistance, when the tip moves over the sample, is clearly visible. During interval (i) the resistance rises by $\Delta R \approx 10$ k Ω . In return the resistance drops again, when no force is applied. During interval (ii) the resistance increases by values up to $\Delta R \approx 24$ k Ω . This reversible effect is very pronounced in Fig. 3. The same resistance is reached many times by nanomachining even after a longer pause between interval (ii) and (iii).

We again attribute this observed reversible change in the resistance to induced and moving dislocations as before. As this setup is a three terminal device we have to take a contact resistance into account. By this we again find quite good qualitative agreement assuming a classical se-

ries of resistances according to the geometry of the sample.

In conclusion, we have shown *in-situ* measurements of the resistance of mesoscopic graphite being nanomachined with a diamond coated AFM tip. In doing so we find a reversible change in the electrical resistance. We attribute this effect to induced dislocations that lead to an increased resistance. At room temperature these dislocations can easily move to the edges of the graphite flake leading to reversible resistance changes. After processing a sample with the AFM tip a couple of times the resistance changes permanently, i.e. bonds inside the graphite are broken permanently.

-
- ¹ R. Magno and B. R. Bennett, *Appl. Lett. Phys.* **70**, 1855 (1997).
- ² H. W. Schumacher, U. F. Keyser, U. Zeitler, and R. J. Haug, *Appl. Phys. Lett.* **75**, 1107 (1999).
- ³ J. Regul, U. F. Keyser, M. Paesler, F. Hohls, U. Zeitler, R. J. Haug, A. Malav, E. Oesterschulze, D. Reuter, and A. D. Wieck, *Appl. Phys. Lett.* **81**, 2023 (2002).
- ⁴ B. Irmer, R. H. Blick, F. Simmel, W. Gdel, H. Lorenz, and J. P. Kotthaus, *Appl. Lett. Phys.* **73**, 2051 (1998).
- ⁵ B. Oezylmaz, P. Jarillo-Herrero, D. Efetov, and P. Kim, *Appl. Lett. Phys.* **91**, 192107 (2007).
- ⁶ C. Stampfer, J. Güttinger, F. Molitor, D. Graf, T. Ihn, and K. Ensslin, *Appl. Phys. Lett.* **92**, 012102 (2008).
- ⁷ S. Russo, J. B. Oostinga, D. Wehenkel, H. B. Heersche, S. S. Sobhani, L. M. Vandersypen, and A. F. Morpurgo, arXiv:0711.1508 (unpublished).
- ⁸ K. S. Novoselov, A. K. Geim, S. V. Morozov, D. Jiang, Y. Zhang, S. V. Dubonos, I. V. Grigorieva, and A. A. Firsov, *Science* **306**, 666 (2004).
- ⁹ Y. Zhang, Y.-W. Tan, H. L. Stormer, and P. Kim, *Nature* **438**, 201 (2005).
- ¹⁰ K. S. Novoselov, Z. Jiang, Y. Zhang, S. V. Morozov, H. L. Stormer, U. Zeitler, J. C. Maan, G. S. Boebinger, P. Kim, and A. K. Geim, *Science* **315**, 1379 (2007).
- ¹¹ A. K. Geim and K. S. Novoselov, *Nature Materials* **6**, 183 (2007).
- ¹² NGS Naturgraphit GmbH.
- ¹³ K. S. Novoselov, D. Jiang, F. Schedin, T. Booth, V. V. Khotkevich, S. V. Morozov, and A. K. Geim, *Proc. Natl. Acad. Sci.* **102**, 10451 (2005).
- ¹⁴ A. Grenall, *Nature* **182**, 448 (1958).
- ¹⁵ G. K. Williamson, *Proc. Roy. Soc.* **257**, 457 (1960).
- ¹⁶ R. L. Powell and G. E. Childs, *American Institute of Physics Handbook* (McGraw-Hill, New York, 1972), pp. 4-142 to 4-160.